TECHNIQUES FOR ROBUST NONLINEAR DELTA-F SIMULATIONS OF BEAMS*

Alex Friedman, John J. Barnard, and David P. Grote
LLNL, P.O. Box 808, Livermore, CA 94551 USA

Abstract

We describe means by which the range of applicability of nonlinear-characteristic δf methods to beams may be enhanced, so as to faithfully describe a sharp-edged beam or a smooth beam whose edge moves by more than its scale length. As others have done, we follow a population of Lagrangian characteristic "marker" particles in the total (equilibrium plus perturbation) field. However, in contrast with usual practice, our marker distribution is not proportional to the physical particle distribution. We introduce "ghost" particles: a population of markers loaded into regions of phase space where the equilibrium f_0 is zero or very small. In addition, we do not numerically evolve either δf or a "weight" w, but rather we use knowledge of the marker positions in phase space and of the functional form of f_0 to evaluate δf anew at each timestep for each marker. We describe the application of our formalism to the model problem of an oscillating displaced beam. We show that marker loading with phase-space density proportional to f_0 leads to inconsistencies, while our modified marker loading is consistent and (for modest displacements) can be statistically "quieter" than conventional particle-in-cell simulation.

1 INTRODUCTION

Nonlinear-characteristic δf methods [1-4] have proven highly effective in the simulation of plasmas. However, the application of δf methods to charged particle beams has proven challenging, despite their early use [1] and recent progress [5]. This has been the case largely because few beam equilibria are known. While axisymmetric equilibria are readily constructed, most beams are non-axisymmetric due to the alternating gradient focusing employed. For such beams the only known equilibrium is the "K-V" distribution [6], which is highly singular and exhibits a number of instabilities which are not present in real beams. Furthermore, beams evolve farther from their equilibrium distribution (f_0) than do most of the neutral plasmas to which δf methods are applied. Beams are bounded; while some have extended spatial tails, many (those with very strong space charge, or near apertures) do not. Beam parameters can change dramatically along an accelerator, and externally-applied forces can have complicated structure. At least in some regions of phase space, the perturbation δf can be large (sometimes infinitely large) relative to f_0.

In this paper we explore means by which the range of applicability of δf methods to beams may be enhanced. Despite the above mentioned difficulties, such methods may still prove to have real utility because the offending regions with large perturbations may be localized, and so integral quantities may be insensitive to such local errors; this must be evaluated on a problem-by-problem basis.

Traditional δf methods, using a marker loading proportional to the physical particle distribution, cannot consistently describe the behavior of a sharp-edged beam undergoing a displacement. We sought revised δf methods which can work even in the extreme limit of a sharp-edged beam. We suggest that two techniques are key. The first is the use of "ghost" particles in a marker distribution not proportional to f_0, a technique anticipated in earlier δf work [2] but apparently never used for beams. The second is the use of marker coordinates and the functional form of f_0 to evaluate δf anew at each timestep for each marker, rather than evolving δf in time. This saves the solution of an ODE for each particle, with its attendant errors and possible timestep constraints. It follows a comment by Aydemir [3] and is in contrast with what seems to be common practice in the use of δf methods. These methods should also work well when the edge of a smooth-edged beam moves by more than its characteristic density fall-off scale length, typically the thermal Debye length.

In the following sections of this paper we describe our formalism; the model problem of an oscillating displaced beam in slab geometry; results for a water-bag distribution in the zero-space-charge limit; and results for a Maxwell-Boltzmann distribution for a space-charge-dominated beam. Finally, we offer closing comments.

2 FORMALISM

The physical distribution f(x,v) integrates to the total number of particles, N:

$$N = \int dx\ dv\ f(x,v) \tag{1}$$

An idealized marker distribution $f_m(x,v)$ — the number of markers per unit phase space volume — integrates to the total number of markers, N_m:

$$N_m = \int dx\ dv\ f_m(x,v) \tag{2}$$

We consider f and f_m to be continuous and finite; below, we discuss the correspondence to a set of discrete markers {i}. The Vlasov equation in the electrostatic limit is:

$$\frac{df}{dt} = \frac{\partial f}{\partial t} + v \cdot \nabla f + \frac{q}{m} E \cdot \nabla_v f = 0 \tag{3}$$

and the evolution equation for the perturbation $\delta f = f - f_0$ is:

$$\frac{d}{dt}\delta f = -\frac{df_0}{dt} = -\frac{q}{m}\delta \mathbf{E} \cdot \nabla_v f_0 \tag{4}$$

(we need not time-advance this!). The unperturbed and perturbation particle number densities are:

$$n_0(x) = \int dv\, f_0(x,v) \qquad \delta n(x) = \int dv\, \delta f(x,v) \tag{5}$$

The total field, used to advance the markers via a split-leapfrog step, is $E = E_0 + \delta E$. The probability densities are $p(x,v) = f(x,v)/N$ and $p_m(x,v) = f_m(x,v)/N_m$; these integrate to unity and represent the likelihood that a single particle or marker is to be found in a given unit volume of phase space. We define two sets of constants along the marker trajectories:

$$f_i = f(x_i, v_i); \qquad f_{mi} = f_m(x_i, v_i)\ . \tag{6}$$

Assigning a phase-space volume $V_{mi} = 1/f_{mi}$ to each marker, the "Klimontovich" distribution is:

$$\begin{aligned} f_{K\lim}(x,v) &= \sum_{i=1}^{N_m} f(x_i,v_i) V_{mi} \delta(x-x_i)\delta(v-v_i) \\ &= \sum_{i=1}^{N_m} \frac{f_i}{f_{mi}} \delta(x-x_i)\delta(v-v_i) \end{aligned} \tag{7}$$

The moment of a quantity A is approximated by

$$\begin{aligned} \langle A \rangle &= \frac{1}{N} \int A(x,v) f(x,v) dx dv \\ &\approx \frac{1}{N} \int A(x,v) f_{K\lim}(x,v) dx dv \end{aligned} \tag{8}$$

giving:

$$\langle A \rangle \approx \frac{1}{N} \sum_{i=1}^{N_m} A(x_i,v_i) \frac{f_i}{f_{mi}}\ . \tag{9}$$

Similarly, the Klimontovich distribution for markers is:

$$f_{m,K\lim}(x,v) = \sum_{i=1}^{N_m} \delta(x-x_i)\delta(v-v_i)\ . \tag{10}$$

We replace spatial delta functions $\delta(x-x_i)$ with the particle "shape function" $S(x_j - x_i)/\Delta x$, where Δx is the cell size. The charge density in grid cell j in a conventional PIC code is:

$$n_j = \sum_i \frac{N}{N_m} \frac{S(x_j - x_i)}{\Delta x} \tag{11}$$

or, for non-uniform particle weighting:

$$n_j = \sum_i \frac{N}{N_m} \frac{p_i}{p_{mi}} \frac{S(x_j - x_i)}{\Delta x} = \sum_i \frac{f_i}{f_{mi}} \frac{S(x_j - x_i)}{\Delta x}\ , \tag{12}$$

where $p_i = f_i/N$ and $p_{mi} = f_{mi}/N_m$ remain constant along trajectories, just as do f_i and f_{mi}. In a δf calculation, our form for the perturbed charge density is:

$$\delta n_j = \sum_i \left(\frac{f_i - f_0\left(x_i(t), v_i(t)\right)}{f_{mi}} \right) \frac{S(x_j - x_i)}{\Delta x} \tag{13}$$

or, introducing a perturbed "weight" for each particle i,

$$\delta n_j = \sum_i w_i \frac{S(x_j - x_i)}{\Delta x}, \tag{14}$$

where

$$w_i(t) = \frac{N}{N_m} \frac{\delta f_i}{f_i} \frac{p_i}{p_{mi}} = \frac{\delta f\left(x_i(t), v_i(t)\right)}{f_{mi}}\ . \tag{15}$$

This matches Aydemir's eq. (19), noting the differing notation, *e.g.*, his "N" is our N_m. It also matches Parker and Lee's eq. (7), again with differences in notation. It differs from the common expression for PIC-like loading in that the denominator is f_{mi} instead of f_i.

Each particle makes a contribution to δn proportional to $(f_i - f_0)/f_{mi}$. Here, the first term simply advects around with the markers and always contributes positively to δn. The second term is zero or contributes negatively to δn, as necessary to cancel the unwanted equilibrium n_0 in regions not currently being occupied by the beam.

Direct evaluation is simpler than time-evolution. Still following Aydemir, from the equation for dδf/dt we find:

$$\frac{dw_i}{dt} = -\left[\frac{1}{f_{mi}} \frac{df_0}{dt} \right]_{(x,v)=(x_i,v_i)}\ . \tag{16}$$

As Aydemir notes, it is "under normal circumstances" not necessary to solve this, since δf_i or w_i at any time can readily be computed from:

$f_0(x_i,v_i)$ (by direct evaluation of the specified f_0),
f_i (constant, by Liouville's theorem), and
f_{mi} (constant, by Liouville's theorem).

This is a considerable advantage for beams, where f_0 may change radically along the exact orbits. Two quantities (f_i and f_{mi}) need to be stored for direct evaluation, just as two quantities (w_i and f_{mi}) need to be stored for time-evolution. Only in the case of PIC-like loading of markers, where f_i/f_{mi} is the same number for all particles, is it possible to dispense with one of these stored quantities. This savings is unlikely to be significant.

3 MODEL PROBLEM

A sheet beam subjected at t = 0 to a constant, uniform sideways force illustrates the relevant principles. For the moment, we assume infinitesimal space charge, using the accumulated number density only as a measure of the effectiveness of our methods (this assumption will be relaxed in Section 5, below). The beam moves with constant axial velocity $v_z = v_0$. The transverse force balance is between thermal pressure and an applied linear confining field $E_0(x) = -E'_0 x$. The betatron frequency is ω, where $\omega^2 = qE'_0/m$. A "slice" of particles passes through z = 0 at time t = 0, at which time a transverse electric field δE is applied; the effect is to shift the bottom of the electrostatic potential well by a distance $x_c = q\delta E/m\omega^2 = \delta E/E'_0$. See Figure 1. Since there is no damping, the beam's centroid overshoots to $2x_c$, and the system rings forever at frequency ω. See Figure 2, which shows an extreme case. In phase space, the beam precesses around $(x_c,0)$; see Figures 3 and 4.

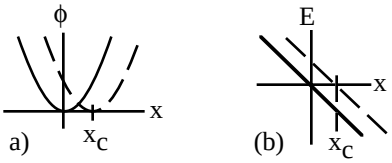

Figure 1. For the model problem in the zero-space-charge limit, (a) potential and (b) electric field vs. transverse coordinate x. Solid line is unperturbed, dashed perturbed.

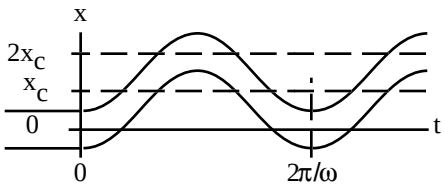

Figure 2. Beam motion in {x,t} space for model problem.

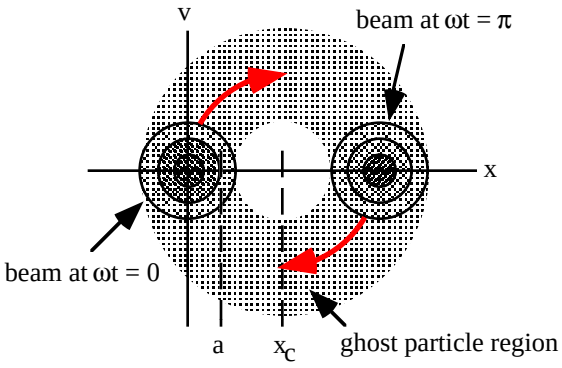

Figure 3. Beam motion in phase space for model problem.

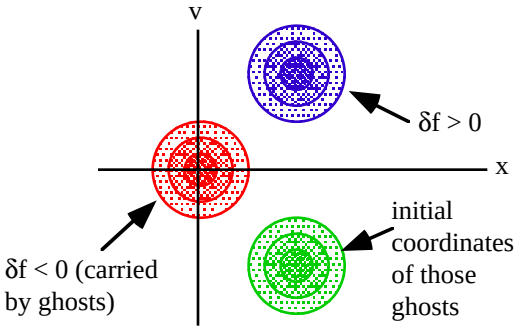

Figure 4. Phase space at ωt = π/2 for model problem.

4 WATERBAG DISTRIBUTION IN ZERO SPACE CHARGE LIMIT

A waterbag distribution illustrates the issues. This is a "sharp-edged" equilibrium with negligible space charge. We set the phase space density constant out to a cutoff circle at energy h_0 in the phase space {ωx,v}:

$$f_0(x,v) = \begin{cases} \dfrac{N\omega}{2\pi h_0}, & v^2 + \omega^2 x^2 \le 2h_0 \\ 0, & v^2 + \omega^2 x^2 > 2h_0 \end{cases}, \qquad (17)$$

leading to a particle density:

$$n_0(x) = \begin{cases} \dfrac{N\omega}{\pi h_0}\sqrt{2h_0 - \omega^2 x^2}, & |x| \le \dfrac{\sqrt{2h_0}}{\omega} \\ 0, & |x| > \dfrac{\sqrt{2h_0}}{\omega} \end{cases}. \qquad (18)$$

The displacement of this distribution cannot be simulated consistently with a δf simulation using PIC-like loading.

We consider two marker loadings which afford consistent δf-derived densities for the waterbag problem. For both, the boundaries of the marker region are time-invariant, since E is time-invariant and markers are uniformly loaded along characteristics (in the presence of the displacing force). Loadings such as these only work for negligible space charge. They are:

(1) A "disk" loading, which uniformly populates a "circle" in phase space of radius $r_d = x_c + \sqrt{2h_0}/\omega$ centered at $(x_c,0)$:

$$f_m = N_m / \pi\left(x_c + \sqrt{2h_0}/\omega\right)^2 = \text{const.} \qquad (19)$$

(2) An optimized "annulus" loading, wherein the markers uniformly populate an annulus of outer and inner radii $r_\pm = x_c \pm \sqrt{2h_0}/\omega$ centered at $(x_c,0)$:

$$f_m = N_m / \pi\left[\left(x_c + \sqrt{2h_0}/\omega\right)^2 - \left(x_c - \sqrt{2h_0}/\omega\right)^2\right] = \text{const.} \qquad (20)$$

In carrying out these waterbag tests we were able to take advantage of the fact that the orbits in the applied field are readily computed. Rather than time-stepping as in an actual PIC code, we evaluated marker locations at ωt = π analytically using:

$$x - x_c = (x_0 - x_c)\cos(\omega t) + \frac{v_0}{\omega}\sin(\omega t)$$
$$v = -\omega(x_0 - x_c)\sin(\omega t) + v_0\cos(\omega t) \qquad (21)$$

This is possible because (for this model) the space charge is negligible, used merely as a diagnostic. A 1-d version of area weighting was used; results for nearest-grid-point charge deposition are similar. Best agreement was obtained by using the analytic density averaged over a length Δx centered at each grid point as a reference density; again, differences are minor. Results are shown for conventional PIC, delta-f using PIC-like loading (marker density proportional to f_0), and the two marker loadings described earlier. In all cases, the "physical" particle number $N = 10^9$, number of markers $N_m = 25{,}000$, number of grid cells $n_g = 400$, and limits of the computational domain $x_l = -5$ and $x_h = 15$.

In Figure 5 the density at ωt = π is shown. Note the failure of δf with PIC-like loading to cancel the unwanted zero-order density at the left. The relative error vs. x for $x_c = 0.05$ is shown in Figure 6, and its variation with x_c in Figure 7. Even annulus-loading δf is inferior to PIC beyond $x_c \sim 0.4$, though it remains consistent.

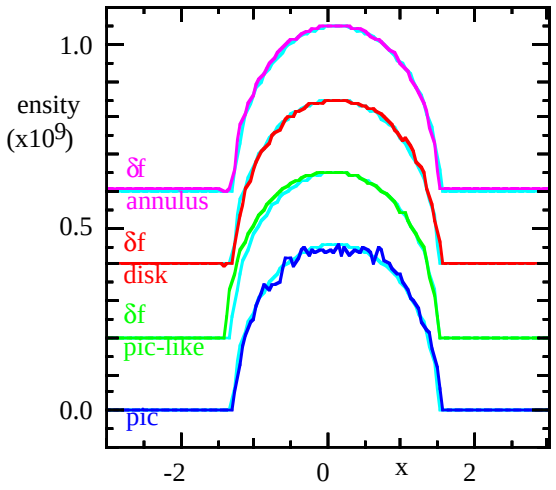

Figure 5. Waterbag problem: density vs. x at $\omega t = \pi$ for $x_c = 0.05$; an offset between the ordinates aids clarity. The analytic density is shown in light color.

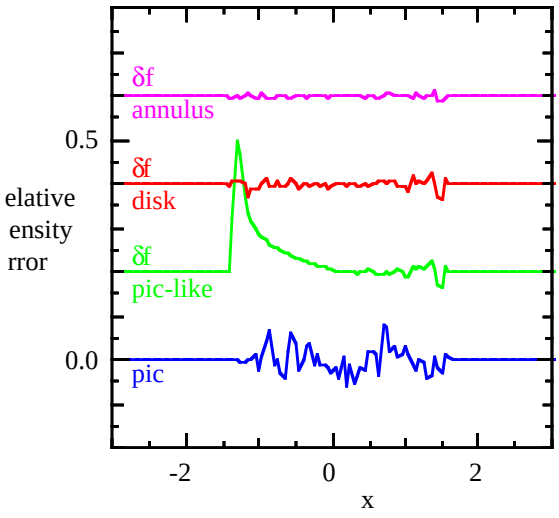

Figure 6. Density error normalized to peak density vs. x at $\omega t = \pi$ (note offset)

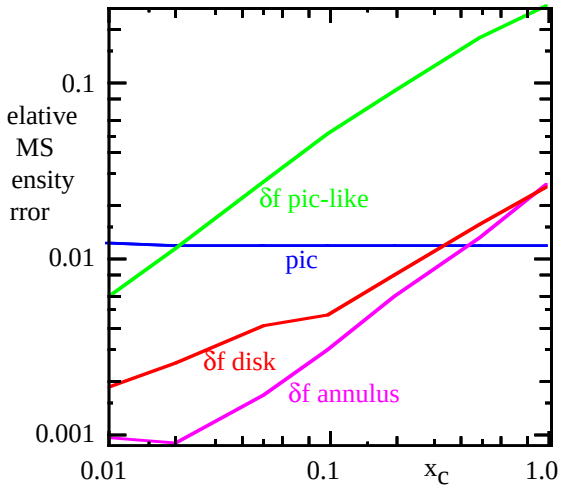

Figure 7. RMS over x of density error (normalized to peak density) vs. offset x_c at $\omega t = \pi$.

5 MAXWELL-BOLTZMANN DISTRIBUTION WITH SPACE CHARGE

When space charge is not negligible, marker loading requires care. E varies with time, and loadings "centered" about x_c are not stationary. For the model problem, quasi-stationary marker distributions can be obtained by loading markers uniformly along the equilibrium orbits in the unperturbed field. Since the applied perturbation field shifts all orbits (physical and marker) by the same phase-space offset, the marker distribution is stationary about the moving beam centroid. If the marker distribution is made "large enough," the phase-space area vacated by the precessing beam is always "well-covered" with markers and the unwanted n_0 is canceled. However, such loadings are in general less "efficient" than the annulus loading that works well for negligible space charge.

We are testing various marker loadings; here we use a rescaled PIC-like loading: $x_j \Leftarrow [(2x_c+a_0)/a_0]x_j$; $v_j \Leftarrow [2x_c\omega_{\beta 0}/v_{th}]v_j$. The distribution value f_{mj} for each marker j is reduced relative to that of PIC-like loading by the product of the factors in [ ]. This sub-optimal "blob" loading is not uniform along unperturbed orbits, and the marker distribution is not quasi-stationary. Nonetheless, it covers the required phase space. Work in progress (to be described in a future publication) indicates that improved results (in some cases significantly better than those of PIC) are obtainable from a cut-off uniform marker loading.

We have done PIC and δf simulations of a space-charge-dominated Maxwell-Boltzmann (M-B) sheet beam. The equilibrium, which must be computed numerically, is:

$$f = f_0 \exp\left(-\frac{H_\perp}{k_B T_\perp}\right) = f_0 \exp\left(-\frac{mv_x^2/2 + q\phi_{tot}(x)}{k_B T_\perp}\right). \quad (22)$$

We chose a strongly tune-depressed case, with ratio of depressed to undepressed phase advance $\sigma/\sigma_0 = 0.2$. Also: $a_0 = 0.01$ m (edge position of RMS-equivalent uniform beam); $n_x = 512$ (number of cells across x); $x_c = 0.002$ m (offset of equilibrium x due to displacing force); $n_m = 32768$ (number of markers); $\Delta t/\tau_{\beta 0} = 1/16$ or 1/32 (the latter gives visibly better results).

In figure 8 the initial PIC and marker locations are shown; the "ghost" region is sizable (these figures are best viewed online, in color). In Figure 9 the initial PIC beam is again shown, now overlaid with the PIC beam and the markers at $\omega_{\beta 0} t = \pi$. In Figure 10 the markers with the most significant perturbations are displayed in dark colors (for clarity, more markers were used in this run; when a smaller time step is used, the regions become roughly circular). In Figure 11 the profile at $\omega_{\beta 0} t = \pi$ is shown for the three methods. The failure of δf with PIC-like loading is evident. When the modified loading is used, δf is smoother than PIC over most of the beam, but noisier at the beam edges (improved loadings can fix this).

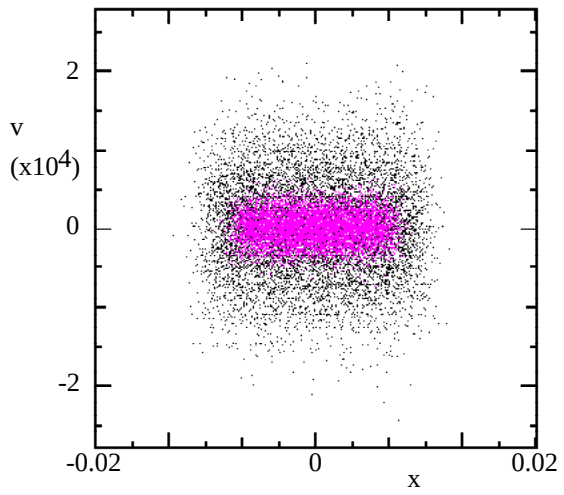

Figure 8. Initial PIC beam (magenta) and markers (black) for "blob" loading of M-B beam with space-charge.

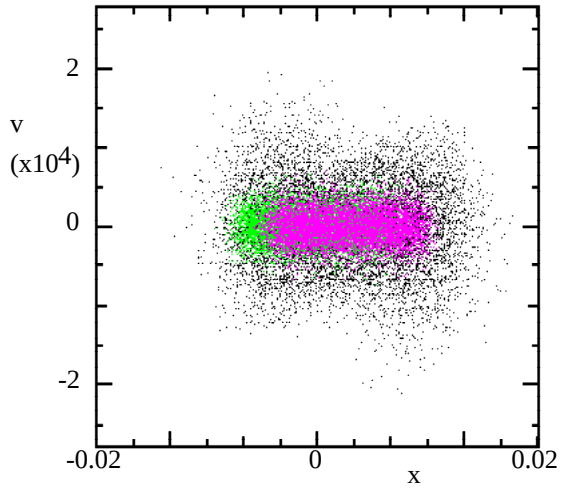

Figure 9. Initial PIC beam (green), PIC beam at $\omega_{\beta 0} t = \pi$ (magenta), and markers at $\omega_{\beta 0} t = \pi$ (black).

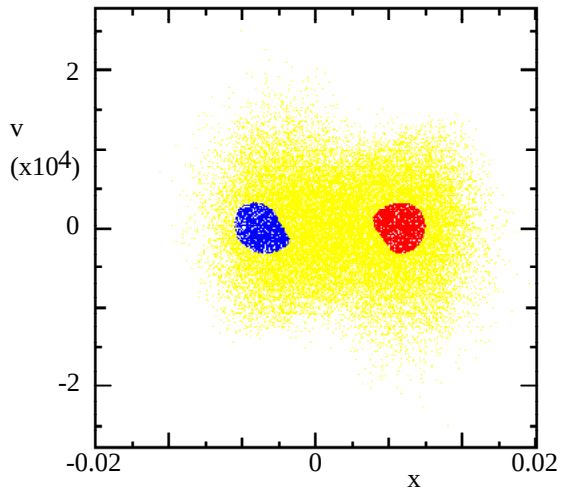

Figure 10. Markers at $\omega_{\beta 0} t = \pi$; Red denotes $\delta f \geq 0.2\ f_{max}$; blue $\delta f \leq -0.2\ f_{max}$; yellow all other

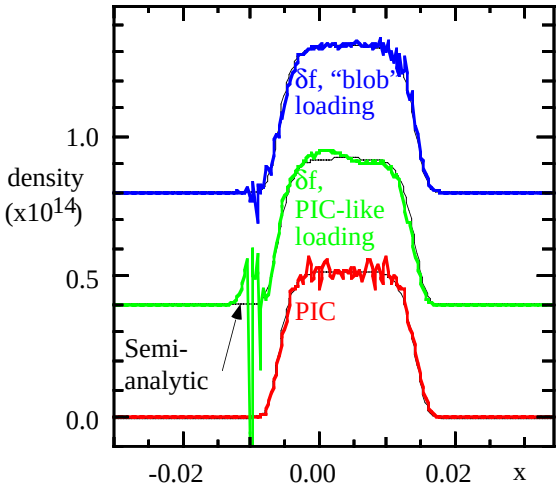

Figure 11. Density profiles at $\omega_{\beta 0} t = \pi$ for M-B beam.

6 DISCUSSION

We have identified δf methods which handle even a sharp-edged beam, and shown that use of PIC-like marker loading leads to inconsistencies in such cases. The K-V distribution is sharp-edged (and singular, in phase space). If δf methods are to be reliably applied to it, great care must be taken to ensure cancellation of undesired n_0 as the thin shell in phase space deforms. This may prove very difficult to do consistently.

Timestep constraints associated with accurately tracking the markers in the total field remain. In many cases these constraints resemble those of PIC, since the marker advance is identical with that of PIC, except that the field solution is unconventional. In other cases the constraints may be more severe, since (as was shown) markers must sometimes be followed in regions of phase space that remain unpopulated in PIC calculations.

Because of their difficulties when the beam evolves considerably, we should not expect these methods (at least in their present form) to become a general replacement for PIC beam simulations. Their extra "quietness" makes these robust δf variants attractive for special purposes, *e.g.*, the detailed study of particular modes on a beam.

REFERENCES

* Work performed under the auspices of the U.S. D.O.E. by LLNL under contract W-7405-ENG-48.

[1] W. M. Fawley, *BAPS* **27**, 1034 (Oct. 1982).

[2] S. E. Parker and W. W. Lee, *Phys. Fluids* B **5**(1), 77-86 (1993).

[3] A. Y. Aydemir, *Phys. Plasmas* **1**(4), 822-31 (1994).

[4] G. Hu and J. A. Krommes, *Phys. Plasmas* **1**(4), 863-74 (1994).

[5] P. H. Stoltz, R. C. Davidson & W. W. Lee, *Phys. Plasmas* **5**, 1998 (in press).

[6] I. Kapchinskij and V. Vladimirskij, in *Proc. Int. Conf. on High Energy Accel. and Instrumentation* (CERN Scientific Information Service, Geneva, 1959), p. 274.